Distributionally Robust Co-optimization of Transmission Network Expansion Planning and Penetration Level of Renewable Generation

Jingwei Hu, Xiaoyuan Xu, Hongyan Ma, and Zheng Yan

***Abstract*—Transmission network expansion can significantly improve the penetration level of renewable generation. However, existing studies have not explicitly revealed and quantified the trade-off between the investment cost and penetration level of renewable generation. This paper proposes a distributionally robust optimization model to minimize the cost of transmission network expansion under uncertainty and maximize the penetration level of renewable generation. The proposed model includes distributionally robust joint chance constraints, which maximize the minimum expectation of the renewable utilization probability among a set of certain probability distributions within an ambiguity set. The proposed formulation yields a two-stage robust optimization model with variable bounds of the uncertain sets, which is hard to solve. By applying the affine decision rule, second-order conic reformulation, and duality, we reformulate it into a single-stage standard robust optimization model and solve it efficiently via commercial solvers. Case studies are carried on the Garver 6-bus and IEEE 118-bus systems to illustrate the validity of the proposed method.**

***Index Terms*—Affine decision rule, distributionally robust optimization, joint chance constraint, renewable generation, transmission network expansion planning.**

NOMENCLATURE

A. Indices

g	Index of thermal generator
i, j	Indices of node
k	Index of renewable generator
l	Index of corridor
m	Index of transmission line
t	Index of time interval

B. Sets

Ω	Set of candidate corridors
$\mathcal{T}, \mathcal{N}, \mathcal{G}, \mathcal{K}$	Sets of time, nodes, thermal generators, and renewable generators
$\mathcal{N}_i, \Omega_i, \mathcal{G}_i, \mathcal{K}_i$	Sets of nodes, candidate corridors, thermal generators, and renewable generators connected to node i
$\mathcal{N}_l$	Set of nodes connected by transmission lines over corridor l
$\mathcal{M}_l$	Set of transmission lines over corridor l

C. Parameters

δ	Weight factor representing system planners' willingness for renewable utilization
$\theta_i^{\min}, \theta_i^{\max}$	The minimum and maximum phase angles of node i
$\mu_{k,t}, \sigma_{k,t}$	Empirical mean and variance of power output of renewable generator k at time t
c_l	Investment cost of each line over corridor l
$F_l^{\min}, F_l^{\max}$	The minimum and maximum power flows of transmission lines over corridor l
$n_l^{\min}, n_l^{\max}$	The minimum and maximum numbers of transmission lines over corridor l
$\underline{p}_g^{\text{gen}}, \bar{p}_g^{\text{gen}}$	The minimum and maximum outputs of thermal generator g
u_0	Lower bound of the minimum possibility with which system can fully accommodate renewable generation
x_l	Reactance of each line over corridor l

D. Variables

$\alpha_l^{(m)}$	Binary variable representing built/not-built status of the m^{th} line over corridor l
$\theta_{i,t}$	Phase angle of node i at time t
$\xi_{k,t}$	Power output of renewable generator k at time t
ξ_t	Power output of all renewable generators at time t
$\xi_{k,t}^{\text{L}}, \xi_{k,t}^{\text{U}}$	The minimum and maximum outputs of renewable generator k at time t that power system can fully accommodate
$\xi_t^{\text{L}}, \xi_t^{\text{U}}$	The minimum and maximum outputs of all renewable generators at time t that power sys-

Manuscript received: March 3, 2021; revised: July 21, 2021; accepted: October 27, 2021. Date of CrossChecked: October 27, 2021. Date of online publication: December 8, 2021.

This work was supported by the National Natural Science Foundation of China (No. 52077136).

J. Hu, X. Xu (corresponding author), and Z. Yan are with Key Laboratory of Control of Power Transmission and Conversion of Ministry of Education, Shanghai Jiao Tong University, Shanghai, China (e-mail: jingwei-hu@sjtu.edu.cn; xuxiaoyuan@sjtu.edu.cn; yanz@sjtu.edu.cn).

H. Ma is with Donghua University, Shanghai 201620, China (e-mail: hongyanm@dhu.edu.cn).

DOI: 10.35833/MPCE.2021.000156

tem can fully accommodate

$f_{l,t}^{(m)}$ Power flow of the m^{th} line over corridor l at time t

$f_{l,t}$ Sum of power flow of each line built over corridor l at time t

$p_{i,t}^{dem}$ Power demand of node i at time t

$p_{g,t}^{\text{gen}}$ Power output of thermal generator g at time t

u The minimum possibility with which system can fully accommodate renewable generation

I. Introduction

THE spatial and temporal mismatches between the renewable energy generation and load centers trigger a series of economic, ecological, and safe problems. To resolve the mismatches, many researchers focus on the transmission network expansion problems (TNEPs), which aim to provide the best way to expand or reinforce the existing transmission networks to adequately balance the forecasting power generations and demand over a given horizon [1]. The TNEPs are challenging to solve due to various uncertainties that operators need to consider. Traditionally, the uncertainties at the demand side draw specific attention because it is considered as the main source of uncertainties. However, the growing penetration level of renewable generation amplifies the uncertainties and needs more consideration [2], [3].

The most widely-used methods to model the uncertainties in TNEPs are stochastic optimization (SO) and robust optimization (RO) approaches [4], [5]. SO minimizes a weighted sum of the total cost related to typical scenarios generated based on a certain probability distribution of the uncertain parameters [6]-[8]. In RO, decisions are made in the worst-case scenario within an uncertain set depicting the uncertain parameters, to ensure that the optimal results are feasible regardless of uncertainties [9], [10]. In a market-based deregulated context, the SO-based [11] - [13] or RO-based [14] TNEP model is applied to optimize the public and private welfare. From the perspective of central planner, reliability and joint planning are popular topics in this field [15]-[17]. In the aspect of joint planning, SO- or RO-based TNEP model is proposed to co-optimize the generation expansion, energy storage expansion, transmission switching, and various flexibility products [18]-[22]. In the aspect of reliability, [23] proposes an SO framework and [24] presents a two-stage RO-based model.

Such SO and RO approaches face challenges in practice [25], [26]. On one hand, it is usually difficult to obtain the exact distributions of random variables, which are necessary for SO and affect the out-of-sample performances of the optimal results. With the increase of scenario numbers, the computation time will increase dramatically with exponential complexity [27]. On the other hand, for the RO approaches, decisions are made considering the worst-case scenario of the uncertain parameters, thus leading to conservative solutions. Besides, this approach employs limited information to construct the uncertainty set, which does not fully utilize the available historical data. For the two-stage RO methods, numerous dual variables or Lagrange multipliers introduced by the reformulation of the second-stage model cause a heavy computational burden [28].

The distributionally robust optimization (DRO) method, as an improved approach, has been put forward to address the aforementioned challenges [29], [30]. A trade-off between the resilience and cost is achieved by minimizing the expectation under the worst-case probability distribution within the ambiguous set predefined based on the historical data [31], [32]. The DRO method is less conservative than the traditional RO method because the former considers the expectation of the worst-case probability distribution rather than the single worst-case scenario. Moreover, it is more reliable than the SO method and utilizes less knowledge of the uncertain parameters instead of assuming that the uncertainties follow prescribed probability distributions [33], [34].

Regarding the current application of DRO to TNEP, [35] proposes a DRO-based TNEP model with multi-scale uncertainties, i.e., long- and short-term uncertainties, considering conditional ambig-uity sets such as economic growth or renewable energy disruption. In [36], a DRO-based TNEP model is proposed considering the post-contingency services where the first-stage problem determines the investment plans and the scheduling of renewable energy post-contingency services. The second-stage problem minimizes the expected cost of corrective actions under various contingencies. Reference [37] applies a DRO tool for TNEP under the $N-k$ security criterion to handle the problem that the probability of contingencies is often unknown and cannot be estimated precisely.

However, current studies on TNEP have not explicitly quantified the renewable energy that a power system can fully accommodate without load shedding or renewable curtailment, which are highly related to investment decisions. For example, to accommodate a higher level of renewable generation, the system planners need to invest in more new transmission lines or strengthen the existing lines to transmit the substantial sustainable energy from the remote areas to load centers. The explicit penetration level is a clear guideline for system planners to seek a trade-off between the renewable utilization and investment costs.

To bridge the research gap between the TNEP and penetration level of renewable energy, we develop a DRO-based co-optimization model for the TNEP under uncertainty, yielding the minimum investment costs and the maximum penetration levels of renewable generation. The definition of the penetration level of renewable generation in this paper consists of two aspects. One is the accommodation range of renewable generation, within which the power system can fully accommodate renewable outputs by power dispatch without load or renewable shedding. The other aspect is the renewable utilization probability, with which the renewable outputs lay within the accommodation range so that the system can fully accommodate them. The main contributions of this paper are fourfold as follows.

1) To our best knowledge, it is the first time to co-optimize the TNEP investment and the penetration level of renewable generation considering the distributionally robust joint chance constraints. On one hand, the optimal penetra-

tion level of renewable generation gives an explicit guideline for renewable development while keeping the power system away from load shedding or wind power curtailment. On the other hand, the distributionally robust joint chance constraints depict a trade-off between the investment cost and renewable utilization with clear physical meanings in a moderately conservative way.

2) The proposed model is originally a two-stage DRO formulation. It is noted that the distributionally robust joint chance constraint is nonconvex and the stochastic bounds are variables instead of parameters as commonly used in literature. Thus, the application of duality is not straightforward. In this paper, we reformulate the distributionally robust joint chance constraint into a second-order conic formulation. And we substitute the stochastic variable with a combination of its lower bound variables and auxiliary variables to further apply duality. Finally, the proposed model is reformulated to a single-stage RO model and is efficiently solved via commercial solvers.

3) We demonstrate the validity and scalability of the proposed method in Garver 6-bus and IEEE 118-bus systems. The testing results show that the proposed method obtains the minimum investment cost and the maximum penetration level of renewable generation under a predefined weight factor, which represents the system planners' willingness for renewable utilization. Besides, the proposed method is less conservative compared with the traditional RO method. Moreover, the proposed method shows its scalability in a large system test.

The rest of this paper is organized as follows. Section II gives the detailed mathematical formulation of the proposed co-optimization model. In Section III, we present the solution technique used to reformulate the proposed two-stage distributionally robust model into a single-stage standard robust model. In Section IV, we carry out case studies on the Garver 6-bus and IEEE 118-bus systems and compare the proposed method with the traditional RO method. The results show the validity and scalability of the proposed method. Finally, we give the conclusions in Section V.

II. Mathematical Formulation

To give a clear guideline for system planners to seek a trade-off between the penetration level of renewable generation and investment cost, we formulate a co-optimization model considering the renewable uncertainty. In this section, we first give the objective function of the proposed model and then introduce the first- and second-stage constraints. Among them, adjustable distributionally robust joint chance constraints are noted in detail. It should be emphasized that this co-optimization model differs from general two-stage distributionally robust models in that the bounds of the uncertainty sets are decision variables instead of known parameters.

A. Objective Function

The objective function (1) aims to minimize the investment cost and maximize the penetration level of renewable generation under a predefined weight factor, which is expressed as:

$$\min_{\alpha_l^{(m)},\, u,\, \xi_{k,t}^{\mathrm{L}},\, \xi_{k,t}^{\mathrm{U}}} \left(\sum_{l\in\Omega} \sum_{m=n_l^{\min}+1}^{n_l^{\max}} c_l \alpha_l^{(m)} - \delta u \right) \tag{1}$$

It is noted that operational costs are usually considered in the objective function of TNEP models. The reason why they are not considered in (1) is that this paper focuses on exploring the penetration level of renewable generation, which is different from the traditional TNEP model. The modeling of accommodation ranges has implicitly incorporated the wind power curtailment instead of setting the load/renewable shedding costs as a penalty in the objective function. Moreover, this paper aims to highlight the relationship between the transmission capacity and the penetration level of renewable generation. Operators of the networks pay more attention to minimizing the investment cost of transmission lines than to minimizing the operational costs. Therefore, the generation-related terms have been simplified.

B. The First-stage Constraints

The first-stage constraints restrict the first-stage variables $\alpha_l^{(m)}$, which are optimized before the uncertainty realization.

$$\alpha_l^{(m)} \in \{0,1\} \quad \forall l \in \Omega, \forall m \in \mathcal{M}_l \tag{2}$$

$$n_l^{\min} \le \sum_{m=1}^{n_l^{\max}} \alpha_l^{(m)} \le n_l^{\max} \quad \forall l \in \Omega \tag{3}$$

$$\alpha_l^{(m)} \le \alpha_l^{(m-1)} \quad \forall l \in \Omega, \forall m \in \mathcal{M}_l \tag{4}$$

Constraint (2) represents the built/not-built status of each line, and binary variable $\alpha_l^{(m)}=1$ if the m^{th} line over corridor l is built; otherwise, $\alpha_l^{(m)}=0$. Constraint (3) ensures the minimum and maximum numbers of transmission lines over each corridor. Constraint (4) represents the sequential building order of new lines.

C. The Second-stage Constraints

The second-stage constraints are activated after the uncertainty realization, thus involving the uncertain variables $\xi_{k,t}$. Accordingly, some system operating variables, such as the power flows, phase angles, and thermal generation outputs, are regarded as the function of $\xi_{k,t}$. In this context, parts of the second-stage constraints are written as:

$$f_{l,t}(\xi_{k,t}) = \sum_{m=1}^{n_l^{\max}} f_{l,t}^{(m)}(\xi_{k,t}) \quad \forall l \in \Omega, \forall k \in \mathcal{K}, \forall t \in \mathcal{T} \tag{5}$$

$$F_l^{\min}\alpha_l^{(m)} \le f_{l,t}^{(m)}(\xi_{k,t}) \le F_l^{\max}\alpha_l^{(m)} \quad \forall l \in \Omega, \forall m \in \mathcal{M}_l, \forall k \in \mathcal{K}, \forall t \in \mathcal{T} \tag{6}$$

$$2\theta_i^{\min}(1-\alpha_l^{(m)}) \le \theta_{i,t}(\xi_{k,t}) - \theta_{j,t}(\xi_{k,t}) - x_l f_{l,t}^{(m)}(\xi_{k,t}) \le 2\theta_i^{\max}(1-\alpha_l^{(m)}) \quad \forall i,j \in \mathcal{N}_l, \forall l \in \Omega, \forall m \in \mathcal{M}_l, \forall k \in \mathcal{K}, \forall t \in \mathcal{T} \tag{7}$$

$$\theta_i^{\min} \le \theta_{i,t}(\xi_{k,t}) \le \theta_i^{\max} \quad \forall i \in \mathcal{N}, \forall k \in \mathcal{K}, \forall t \in \mathcal{T} \tag{8}$$

$$p_{g,t}^{\mathrm{gen}}(\xi_{k,t}) + \xi_{k,t} - p_{i,t}^{dem} = \sum_{l\in\Omega_i} f_{l,t}(\xi_{k,t}) \quad \forall g \in \mathcal{G}_i, \forall k \in \mathcal{K}_i, \forall i \in \mathcal{N}, \forall t \in \mathcal{T} \tag{9}$$

$$\underline{p}_g^{\mathrm{gen}} \le p_{g,t}^{\mathrm{gen}}(\xi_{k,t}) \le \bar{p}_g^{\mathrm{gen}} \quad \forall g \in \mathcal{G}, \forall k \in \mathcal{K}, \forall t \in \mathcal{T} \tag{10}$$

Constraint (5) represents the total power flow over the cor-

ridor l. Constraint (6) ensures the power flow of each line is within the capacity limits. Constraint (7) represents the direct current power flow function if $\alpha_l^{(m)}=1$; otherwise, the constraint is relaxed. Constraint (8) ensures the phase angle of each node is within technical bounds. Constraint (9) represents the power balance of each node, comprising the outputs of thermal generators and renewable generators, demand, and nodal power injections. Constraint (10) ensures the outputs of thermal generators lay within technical bounds.

To further deliver the second-stage constraints, we introduce the concept of penetration level of renewable generation and then explain the distributionally robust joint chance constraints.

1) Penetration Levels

Once the transmission investment decisions are made, the penetration level of renewable generation is given, which is $[\underline{\xi}_{k,t}^{\mathrm{L}}, \xi_{k,t}^{\mathrm{U}}]$. The output of renewable generation $\xi_{k,t}$ is the source of uncertainties. Only if the renewable outputs are within the penetration level, the power system can fully accommodate them by power dispatch without sacrificing the system reliability such as load shedding or renewable curtailment. Similar concepts have been discussed in the power system operation field. The Independent System Operator (ISO) in New England firstly puts forward the concept of do-not-exceed (DNE) limits, which indicates the maximum renewable generation ranges that the power grid can accommodate without load or renewable shedding [38].

With the above-mentioned concept of penetration level of renewable generation, the problem of finding the penetration level is formulated as an optimization problem that finds the minimum and maximum output levels of renewable energy while satisfying certain constraints, which is expressed as:

$$\underline{p}_k^{\mathrm{ren}} \le \underline{\xi}_{k,t}^{\mathrm{L}} \le \xi_{k,t}^{\mathrm{U}} \le \bar{p}_k^{\mathrm{ren}} \quad \forall k \in \mathcal{K}, \forall t \in \mathcal{T} \tag{11}$$

Constraint (11) represents that the lower and upper bounds of renewable outputs are between the technical limits $[\underline{p}_k^{\mathrm{ren}}, \bar{p}_k^{\mathrm{ren}}]$.

2) Distributionally Robust Joint Chance Constraints

The modeling of the uncertainty in this paper is based on three aspects. The first aspect is the stochastic outputs of renewable generator, represented by $\xi_{k,t}$. The second one is the probability distribution of the renewable generation based on the historical data, represented by probability distribution $\mathbb{P}$. The third one is a set consisting of a series of probability distributions following the same characteristics, represented by the ambiguity set $\mathcal{D}$.

We first build an ambiguity set $\mathcal{D}$ consisting of probability distribution $\mathbb{P}$ of the renewable outputs $\xi_{k,t}$. The ambiguity set $\mathcal{D}$ has the following two characteristics: ① $\xi_{k,t}$ has the same empirical mean $\mu_{k,t}$ and variance $\sigma_{k,t}^2$; and ② $\xi_{k,t}$ is unimodal about $\mu_{k,t}$, which is referred to:

$$\mathcal{D} := \left\{ \mathbb{P}: \mathbb{E}_{\mathbb{P}}(\xi_{k,t}) = \mu_{k,t}, Var(\xi_{k,t}) = \sigma_{k,t}^2 \quad \forall k \in \mathcal{K}, \ \forall t \in \mathcal{T} \right\} \tag{12}$$

Compared with the unimodality assumption of the joint probability, the unimodality assumption of $\xi_{k,t}$ is weaker and is easier to verify by the historical data. Moreover, the ambiguity set $\mathcal{D}$ yields a second-order conic constraint that needs moderate computational complexity (see Section III).

Proceeding to the distributionally robust joint chance constraints, we need to quantify the probability of the utilization of renewable generation lying within the penetration level [39], i.e.,

$$\inf_{\mathbb{P} \in \mathcal{D}} \mathbb{P}(\xi_t \in [\underline{\xi}_t^{\mathrm{L}}, \xi_t^{\mathrm{U}}]) \ge u \quad \forall t \in \mathcal{T} \tag{13}$$

$$u_0 \le u \le 1 \tag{14}$$

Constraint (13) represents that the renewable outputs lying within the penetration levels are likely to happen with the smallest possibility u so that the system can run without load shedding or renewable curtailment. The lower bound of u is u_0, which is assumed to be 2/3. This assumption is related to the model reformulation applying the second-order conic relaxation and is reasonable because the power system usually requires a high penetration level of renewable energy.

3) Co-optimization Model: Compact Formulation

The co-optimization model comprising (1)-(11), (13), and (14) is cast compactly using the following matrices and vectors, which is expressed as:

$$\min_{\boldsymbol{\alpha}, u, \underline{\boldsymbol{\xi}}^{\mathrm{L}}, \boldsymbol{\xi}^{\mathrm{U}}} (\boldsymbol{c}^{\mathrm{T}}\boldsymbol{\alpha} - \delta u) \tag{15}$$

s.t.

$$\boldsymbol{\alpha} \in \boldsymbol{X} \tag{16}$$

$$\boldsymbol{T}(\boldsymbol{\alpha}) + \boldsymbol{W}\boldsymbol{y}(\boldsymbol{\xi}) \le \boldsymbol{H}\boldsymbol{\xi} \quad \forall \boldsymbol{\xi} \in [\underline{\boldsymbol{\xi}}^{\mathrm{L}}, \boldsymbol{\xi}^{\mathrm{U}}] \tag{17}$$

$$\begin{cases} \inf\limits_{\mathbb{P} \in \mathcal{D}} \mathbb{P}(\boldsymbol{\xi} \in [\underline{\boldsymbol{\xi}}^{\mathrm{L}}, \boldsymbol{\xi}^{\mathrm{U}}]) \ge u \\ \boldsymbol{P}u \le \boldsymbol{p} \end{cases} \tag{18}$$

$$\begin{cases} \boldsymbol{Q}\underline{\boldsymbol{\xi}}^{\mathrm{L}} \le \boldsymbol{q} \\ \boldsymbol{R}\boldsymbol{\xi}^{\mathrm{U}} \le \boldsymbol{r} \end{cases} \tag{19}$$

where vector $\boldsymbol{\alpha}$ refers to the first-stage decision variables representing transmission network investment decisions; vector $\boldsymbol{c}$ represents the coefficients in the objective function (15); u is a decision variable related to the minimum utilization probability of renewable generation and is adjusted by δ to optimize the trade-off between the cost and the renewable utilization; and vector $\boldsymbol{y}(\boldsymbol{\xi})$ represents the second-stage decision variables including the outputs of thermal generators, the power flow, and the phase angles. Constraint (16) ensures $\boldsymbol{\alpha}$ is binary to represent the built/not-built status of each candidate transmission line. Constraint (17) is related to the operating constraints with uncertainty. The distributionally robust joint chance constraints are represented by (18). Constraint (19) represents the restrictions on the upper and lower bounds of the uncertainty sets.

III. Solution Techniques

It is noted that the co-optimization model formulated in Section II cannot be easily solved owing to the variable bounds of the uncertain sets, which are decision variables instead of known parameters, and the distributionally robust joint chance constraints. Hence, in this section, we first give the solution techniques to reformulate the distributionally robust joint chance constraints and the variable bounds of the

uncertain sets. And then we transform the two-stage robust model into a single-stage model using the standard robust technique, which yields a solvable conservative approximation model.

A. Affine Decision Rules

Given the outputs of renewable energy, the second-stage decision variables are represented by the affine decision rules as:

$$\boldsymbol{y}(\boldsymbol{\xi})=\boldsymbol{B}\boldsymbol{\xi}+\boldsymbol{b} \tag{20}$$

where variables $\boldsymbol{B}$ and $\boldsymbol{b}$ represent the responses of corresponding operating variables to the renewable outputs.

This approximation physically represents the system corrective actions after uncertainty realization. In this context, the second-stage constraints given in Section II also include:

$$p_{g,t}^{\mathrm{gen}}(\xi_t)=\sum_{k\in\mathcal{K}}(B_{g,k,t}\xi_{k,t}+b_{g,k,t}) \quad \forall g\in\mathcal{G},\forall t\in\mathcal{T} \tag{21}$$

$$f_{l,t}^{(m)}(\xi_t)=\sum_{k\in\mathcal{K}}(B_{l,k,t}\xi_{k,t}+b_{l,k,t}) \quad \forall l\in\Omega,\forall t\in\mathcal{T} \tag{22}$$

$$\theta_{i,t}(\xi_t)=\sum_{k\in\mathcal{K}}(B_{i,k,t}\xi_{k,t}+b_{i,k,t}) \quad \forall i\in\mathcal{N},\forall t\in\mathcal{T} \tag{23}$$

By applying the affine decision rule, the searching space of the optimization problem is restricted to a recourse function and thus yields a conservative approximation that requires moderate computational solving time.

B. Reformulation of Distributionally Robust Joint Chance Constraints

The distributionally robust joint chance constraints in Section II are nonconvex and difficult to apply in practice. In this subsection, we reformulate the constraint (18) into a second-order conic formulation using the Bonferroni approximation, Gauss inequality, and second-order conic relaxation technique, which is expressed as:

$$\left\|\begin{bmatrix}\sqrt{8/3}\\ v_{k,t}-z_{k,t}\end{bmatrix}\right\|_2\le v_{k,t}+z_{k,t} \quad \forall k\in\mathcal{K},\forall t\in\mathcal{T} \tag{24}$$

$$\left\|\begin{bmatrix}g_{k,t}-1\\ 2z_{k,t}\end{bmatrix}\right\|_2\le g_{k,t}+1 \quad \forall k\in\mathcal{K},\forall t\in\mathcal{T} \tag{25}$$

$$\sigma_{k,t}v_{k,t}\le\mu_{k,t}-\xi_{k,t}^{\mathrm{L}} \quad \forall k\in\mathcal{K},\forall t\in\mathcal{T} \tag{26}$$

$$\sigma_{k,t}v_{k,t}\le\xi_{k,t}^{\mathrm{U}}-\mu_{k,t} \quad \forall k\in\mathcal{K},\forall t\in\mathcal{T} \tag{27}$$

$$\sum_{k\in\mathcal{K}}g_{k,t}\le 1-u \quad \forall t\in\mathcal{T} \tag{28}$$

$$g_{k,t},v_{k,t},z_{k,t}\ge 0 \quad \forall k\in\mathcal{K},\forall t\in\mathcal{T} \tag{29}$$

where $g_{k,t}$, $v_{k,t}$, and $z_{k,t}$ are auxiliary variables. Detailed proof can be found in Appendix A.

C. Bounds of Uncertainty Sets

To reformulate the variable bounds of the uncertainty sets, we substitute the renewable outputs $\boldsymbol{\xi}$ with $\boldsymbol{\xi}^{\mathrm{L}}+\boldsymbol{E}\boldsymbol{v}$, where $\boldsymbol{E}$ is a diagonal matrix of $\boldsymbol{\xi}^{\mathrm{U}}-\boldsymbol{\xi}^{\mathrm{L}}$; and $\boldsymbol{v}\in[\boldsymbol{0},\boldsymbol{e}]$, and $\boldsymbol{e}$ is a vector of 1. Hence, the constraint (17) is reformulated as:

$$\boldsymbol{T}(\boldsymbol{\alpha})+\boldsymbol{W}(\boldsymbol{B}\boldsymbol{E}\boldsymbol{v}+\boldsymbol{B}\boldsymbol{\xi}^{\mathrm{L}}+\boldsymbol{b})\le\boldsymbol{H}\boldsymbol{\xi}^{\mathrm{L}}+\boldsymbol{H}\boldsymbol{E}\boldsymbol{v} \quad \forall\boldsymbol{v}\in[\boldsymbol{0},\boldsymbol{e}] \tag{30}$$

Furthermore, we substitute the bilinear part $\boldsymbol{BE}$ and $\boldsymbol{B}\boldsymbol{\xi}^{\mathrm{L}}+\boldsymbol{b}$ with $\boldsymbol{S}$ and $\boldsymbol{s}$, respectively. And then (30) is transformed into:

$$\boldsymbol{T}(\boldsymbol{\alpha})+\boldsymbol{W}(\boldsymbol{S}\boldsymbol{v}+\boldsymbol{s})\le\boldsymbol{H}\boldsymbol{\xi}^{\mathrm{L}}+\boldsymbol{H}\boldsymbol{E}\boldsymbol{v} \quad \forall\boldsymbol{v}\in[\boldsymbol{0},\boldsymbol{e}] \tag{31}$$

Next, the standard robust formulation of constraint (31) is rewritten as:

$$\sup_{\boldsymbol{v}\in[\boldsymbol{0},\boldsymbol{e}]}(\boldsymbol{W}\boldsymbol{S}-\boldsymbol{H}\boldsymbol{E})\boldsymbol{v}\le\boldsymbol{H}\boldsymbol{\xi}^{\mathrm{L}}-\boldsymbol{T}(\boldsymbol{\alpha})-\boldsymbol{W}\boldsymbol{s} \quad \forall\boldsymbol{v}\in[\boldsymbol{0},\boldsymbol{e}] \tag{32}$$

Finally, referring to the duality, the equivalent model of (32) is cast as:

$$\boldsymbol{R}\boldsymbol{e}\le\boldsymbol{H}\boldsymbol{\xi}^{\mathrm{L}}-\boldsymbol{T}(\boldsymbol{\alpha})-\boldsymbol{W}\boldsymbol{s} \tag{33}$$

$$\begin{cases}\boldsymbol{R}\ge\boldsymbol{W}\boldsymbol{S}-\boldsymbol{H}\boldsymbol{E}\\ \boldsymbol{R}\ge\boldsymbol{0}\end{cases} \tag{34}$$

D. Reformulated Co-optimization Model: Detailed Formulation

In detail, the co-optimization model in Section II is reduced to a single-stage RO model, which is a mixed-integer second-order cone programming (MISOCP) problem and is rewritten as:

$$\min\left(\sum_{l\in\Omega}\sum_{m=n_l^{\min}+1}^{n_l^{\max}}c_l\alpha_l^{(m)}-\delta u\right) \tag{35}$$

s.t.

$$s_{l,t}=\sum_{m=1}^{n_l^{\max}}s_{l,t}^{(m)} \quad \forall l\in\Omega,\forall t\in\mathcal{T} \tag{36}$$

$$S_{l,k,t}=\sum_{m=1}^{n_l^{\max}}S_{l,k,t}^{(m)} \quad \forall l\in\Omega,\forall k\in\mathcal{K},\forall t\in\mathcal{T} \tag{37}$$

$$F_l^{\min}\alpha_l^{(m)}\le\sum_{k\in\mathcal{K}}\lambda_k^1+s_{l,t}^{(m)} \quad \forall l\in\Omega,\forall m\in\mathcal{M}_l,\forall t\in\mathcal{T} \tag{38}$$

$$\sum_{k\in\mathcal{K}}\gamma_k^1+s_{l,t}^{(m)}\le F_l^{\max}\alpha_l^{(m)} \quad \forall l\in\Omega,\forall m\in\mathcal{M}_l,\forall t\in\mathcal{T} \tag{39}$$

$$\lambda_k^1\le S_{l,k,t}^{(m)},\lambda_k^1\le 0,\gamma_k^1\ge S_{l,k,t}^{(m)},\gamma_k^1\ge 0 \quad \forall l\in\Omega,\forall k\in\mathcal{K},\forall m\in\mathcal{M}_l,\forall t\in\mathcal{T} \tag{40}$$

$$2\theta_i^{\min}(1-\alpha_l^{(m)})\le\sum_{k\in\mathcal{K}}\lambda_k^2+s_{i,t}-s_{j,t}-x_l s_{l,t}^{(m)} \quad \forall i,j\in\mathcal{N}_l,\forall l\in\Omega,\forall m\in\mathcal{M}_l,\forall t\in\mathcal{T} \tag{41}$$

$$\sum_{k\in\mathcal{K}}\gamma_k^2+s_{i,t}-s_{j,t}-x_l s_{l,t}^{(m)}\le 2\theta_i^{\max}(1-\alpha_l^{(m)}) \quad \forall i,j\in\mathcal{N}_l,\forall l\in\Omega,\forall m\in\mathcal{M}_l,\forall t\in\mathcal{T} \tag{42}$$

$$\lambda_k^2\le S_{i,k,t}-S_{j,k,t}-x_l S_{l,k,t}^{(m)} \quad \forall i,j\in\mathcal{N}_l,\forall l\in\Omega,\forall k\in\mathcal{K},\forall m\in\mathcal{M}_l,\forall t\in\mathcal{T} \tag{43}$$

$$\lambda_k^2\le 0 \quad \forall k\in\mathcal{K} \tag{44}$$

$$\gamma_k^2\ge S_{i,k,t}-S_{j,k,t}-x_l S_{l,k,t}^{(m)} \quad \forall i,j\in\mathcal{N}_l,\forall k\in\mathcal{K},\forall l\in\Omega,\forall m\in\mathcal{M}_l,\forall t\in\mathcal{T} \tag{45}$$

$$\gamma_k^2\ge 0 \quad \forall k\in\mathcal{K} \tag{46}$$

$$\theta_i^{\min}\le\sum_{k\in\mathcal{K}}\lambda_k^3+s_{i,t} \quad \forall i\in\mathcal{N},\ \forall t\in\mathcal{T} \tag{47}$$

$$\sum_{k\in\mathcal{K}}\gamma_k^3+s_{i,t}\le\theta_i^{\max} \quad \forall i\in\mathcal{N},\ \forall t\in\mathcal{T} \tag{48}$$

$$\begin{cases} \lambda_k^3 \le S_{i,t} & \forall i \in \mathcal{N},\ \forall k \in \mathcal{K},\ \forall t \in \mathcal{T} \\ \lambda_k^3 \le 0 & \forall i \in \mathcal{N},\ \forall k \in \mathcal{K},\ \forall t \in \mathcal{T} \\ \gamma_k^3 \ge S_{i,t} & \forall i \in \mathcal{N},\ \forall k \in \mathcal{K},\ \forall t \in \mathcal{T} \\ \gamma_k^3 \ge 0 & \forall i \in \mathcal{N},\ \forall k \in \mathcal{K},\ \forall t \in \mathcal{T} \end{cases} \tag{49}$$

$$-\xi_{k,t}^{\mathrm{L}} - s_{g,t} + p_{i,t}^{dem} + \sum_{l \in \Omega_i} \sum_{m=1}^{n_l^{\max}} s_{l,t}^{(m)} = 0 \quad \forall k \in \mathcal{K}_i, \forall g \in \mathcal{G}_i, \forall i \in \mathcal{N},\ \forall t \in \mathcal{T} \tag{50}$$

$$E_{k,t} + S_{i,k,t} - \sum_{l \in N_i} \sum_{m=1}^{n_l^{\max}} S_{l,k,t} = 0 \quad \forall k \in \mathcal{K}_i, \forall i \in \mathcal{N},\ \forall t \in \mathcal{T} \tag{51}$$

$$\underline{p}_g^{\mathrm{gen}} \le \sum_{k \in \mathcal{K}} \lambda_k^4 + s_{g,t} \quad \forall g \in \mathcal{G}, \forall t \in \mathcal{T} \tag{52}$$

$$\sum_{k \in \mathcal{K}} \gamma_k^4 + s_{g,t} \le \bar{p}_g^{\mathrm{gen}} \quad \forall g \in \mathcal{G}, \forall t \in \mathcal{T} \tag{53}$$

$$\begin{cases} \lambda_k^4 \le S_{g,k,t} & \forall g \in \mathcal{G}, \forall k \in \mathcal{K}, \forall t \in \mathcal{T} \\ \lambda_k^4 \le 0 & \forall g \in \mathcal{G}, \forall k \in \mathcal{K}, \forall t \in \mathcal{T} \\ \gamma_k^4 \ge S_{g,k,t} & \forall g \in \mathcal{G}, \forall k \in \mathcal{K}, \forall t \in \mathcal{T} \\ \gamma_k^4 \ge 0 & \forall g \in \mathcal{G}, \forall k \in \mathcal{K}, \forall t \in \mathcal{T} \end{cases} \tag{54}$$

$$(2)\text{-}(4), (11), (24)\text{-}(29)$$

where λ_k^1, γ_k^1, λ_k^2, γ_k^2, λ_k^3, γ_k^3, λ_k^4, γ_k^4, $s_{l,t}^{(m)}$, $s_{l,t}$, $s_{i,t}$, $s_{j,t}$, $s_{g,t}$, $S_{l,k,t}^{(m)}$, $S_{l,k,t}$, $S_{i,k,t}$, $S_{j,k,t}$, $S_{g,k,t}$, and $E_{k,t}$ are auxiliary variables.

Constraints (36) and (37) are reformulated from constraint (5), representing that the total power flow over corridor l is the sum of power flow of each line built over corridor l. Constraints (38)-(40) are reformulated from constraint (6), ensuring the power flow of each line is within the capacity limits. Constraints (41)-(46) are reformulated from constraint (7), representing the direct current power flow equation. Constraints (47)-(49) are reformulated from constraint (8), ensuring the phase angle of each node is within technical bounds. Constraints (50) and (51) are reformulated from constraint (9), representing the power balance of each node. Constraints (52)-(54) are reformulated from constraint (10), ensuring the outputs of thermal generators lay within technical bounds.

IV. Case Study

In this section, we carry out numerical experiments of the proposed model and compare them with the traditional RO method. We use an illustrative example (i.e., the Garver 6-bus system) and a realistic example (i.e., the IEEE 118-bus system). All examples are implemented and solved using the Gurobi API for MATLAB with default parameters. The relative optimality gap tolerance is set to be 0.01%. The simulations are carried out on an Intel Core i5 CPU running at 3.20 GHz with 8 GB of RAM.

We generate a set of wind generation output data via Gaussian distribution, whose mean and variance are set at its predicted value and increases from 10% of the installed capacity by 0.1% as t increases from 1 to T, respectively. The set of data is then divided into two parts: the calibration part and the out-of-sample testing part. For the calibration of ambiguity set, we use the first-part data to calibrate the mean and variance. Next, we solve the proposed model to obtain the optimal accommodation ranges $[\underline{\xi}^{\mathrm{L}^*}, \bar{\xi}^{\mathrm{U}^*}]$ and the optimal investment cost. For the out-of-sample testing part, we apply the second-part data to obtain out-of-sample performances on the utilization probability of renewable energy $\mathbb{P}\{\xi \in (\underline{\xi}^{\mathrm{L}^*}, \bar{\xi}^{\mathrm{U}^*}]\}$. In this paper, we carry out 1000 out-of-sample tests to verify the effectiveness of the proposed method.

In practice, we determine an appropriate δ by trials. Firstly, we roughly estimate the investment cost such as 1×10^6 M$ or 1×10^7 M$, and then set a small δ such as 100 or 1000, which is relatively much smaller than the estimated investment cost. By using the small δ, we obtain an optimal investment cost and an optimal probability of fully accommodating the renewable generation u^*. Now, we have a better knowledge of the investment cost and the renewable utilization probability u. Next, we conduct fine-tuning: setting δ the same as the investment cost. Since the renewable utilization probability u is a value between 0 to 1, usually between 0.6 to 1, the product of δ and u is close to and smaller than the investment cost. Then, by gradually increasing δ by an appropriate step, we obtain a frontier of the investment cost and the renewable utilization probability u. Finally, according to the investment budget and the policy goal of renewable generation utilization, we determine δ to balance the investment cost and penetration level of renewable generation.

A. Illustrative Example: Garver 6-bus System

The initial topology and electric data of the Garver 6-bus system can be found in [40]. In this paper, we use a modified Garver system to illustrate the influences of renewable energy on investment decisions. The topology and parameters are shown in Fig. 1 and Table I, respectively. It is noted that bus 6 is initially isolated. The line parameters of corridor 2-6 and corridor 4-6 refer to the parameters of candidate lines. The minimum and maximum outputs of each generator are set to be 5% and 100% of the nominal outputs, respectively. The maximum number of transmission lines over each corridor is 6. Besides, the construction price per kilometer is 20 k$. The coefficients of wind generation outputs and demand are shown in Fig. 2.

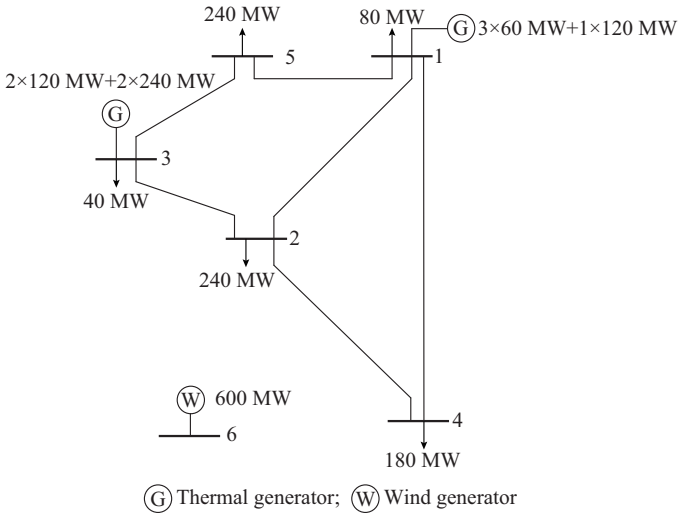

Fig. 1. Topology of modified Garver 6-bus system.

TABLE I
PARAMETERS OF MODIFIED GARVER 6-BUS SYSTEM

Corridor	Length (km)	Reactance (p.u.)	Capacity (MW)
1-2	40	0.04	70
1-4	60	0.06	70
1-5	20	0.02	70
2-3	20	0.02	70
2-4	40	0.04	70
2-6	30	0.03	70
3-5	20	0.02	70
4-6	30	0.03	70

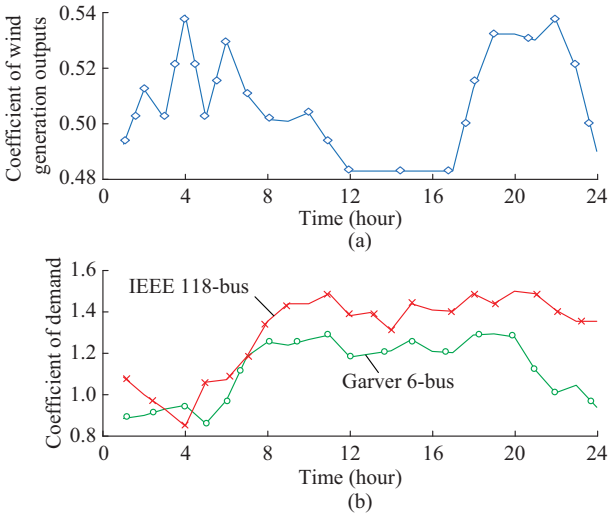

Fig. 2. Coefficients of wind generation outputs and demand. (a) Ratio of wind generation output to nominal value. (b) Ratio of demand to benchmark for modified Garver 6-bus and IEEE 118-bus systems.

In Fig. 3, we exhibit the wind generation outputs from 1000 scenarios with error bars. These error bars represent the mean and variance of wind generation outputs. It can be observed from Fig. 3 that although the wind generation outputs vary, most of them are within a certain range, which can be accommodated with a moderate investment cost.

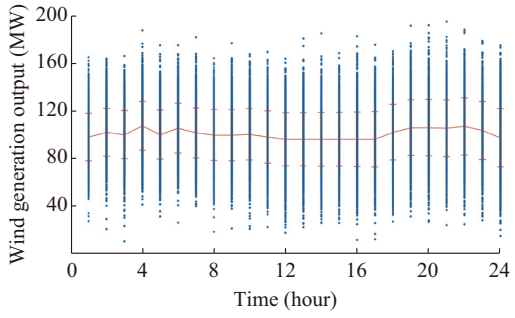

Fig. 3. Distribution of wind generation outputs with error bars.

In the meantime, we can observe that several wind generation outputs depart away from the mean, which requires more transmission lines and more flexible system resources, thereby more investment costs. From the perspective of system planners, the trade-off is necessary when their willingness for renewable accommodation is limited, which means they are not willing to pay too many extra costs for scenarios that seldom exist. Given the proposed method in this paper, the trade-off is easier to decide and the penetration level is more intuitive for reference.

B. Trade-off Between Cost and Accommodation Ranges

The optimal investment plans with proposed DRO method are shown in Table II. As can be observed from Table II, when δ increases, more new lines will be built, thereby yielding higher investment costs. This is because δ represents the weighting factor for renewable utilization, which can be regarded as the willingness of the system to fully accommodate wind generation outputs. The increase of δ means that the system wants to fully accommodate more wind generation outputs, which calls for more new lines for power transmission, thus increasing the investment cost.

TABLE II
OPTIMAL INVESTMENT PLANS FOR GARVER 6-BUS SYSTEM WITH PROPOSED DRO METHOD

δ	Corridor (number of newly-built lines)	Cost (k$)
10000	2-3 (3), 2-6 (4), 3-5 (3), 4-6 (3)	6600
18000	2-3 (4), 2-6 (5), 3-5 (3), 4-6 (3)	7600
100000	2-3 (5), 2-6 (6), 3-5 (3), 4-6 (3)	8600

To demonstrate the trade-off between the investment cost and renewable accommodation ranges, we gradually increase the value of δ and solve the proposed model with each δ to obtain the corresponding accommodation ranges. Because the investment cost does not change continuously, the change of δ may not cause the change of the investment cost every time. For example, when δ changes from 100 to 10000, the investment cost remains the same at 6600 k$. When δ changes from 17000 to 18000, the investment cost changes from 6600 k$ to 7600 k$, which can be regarded as a changing point. To illustrate the results briefly and clearly, we choose those changing points for the exhibition. The trade-off between the investment cost and accommodation ranges is shown in Fig. 4.

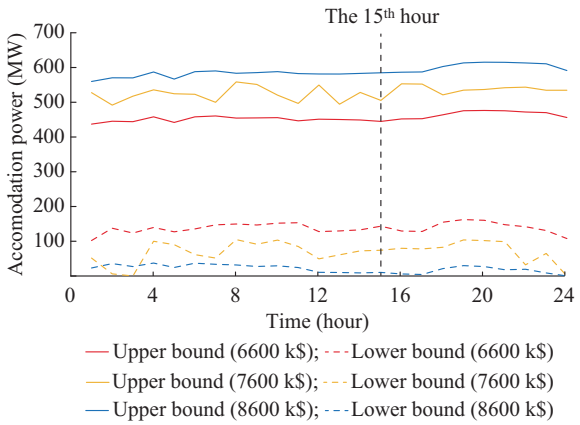

Fig. 4. Trade-off between investment cost and accommodation ranges for Garver 6-bus system.

Taking the cost of 6600 k$ as an example, the space between the upper and lower red lines represents the amount of renewable energy which the system can accommodate without load shedding or wind curtailment. In other words, we need to spend at least 6600 k$ on strengthening the transmission network to accommodate any total wind power output within the interval between two red lines. It is shown that when we increase investment costs, the penetration levels of renewable energy grow. At the 15th hour, the accommodation ranges corresponding to different investment costs of 6600 k$, 7600 k$, and 8600 k$ are 143.42-444.9 MW, 74.22-505.44 MW, and 10.45-584.84 MW, respectively. When the investment increases, more transmission lines will be built, and thus having a more reliable and flexible transmission network. The enhanced transmission network has an improved admissible capacity for renewable energy. It is noted that although the dotted yellow line is lower than the dotted blue line at some times (e.g., at the 2nd and 3rd hours), the interval width of yellow lines is still smaller than that of blue lines. At the 2nd hour, the accommodation ranges corresponding to different investment costs of 7600 k$ and 8600 k$ are 6.23-491.90 MW and 35.73-570.41 MW, respectively. At the 3rd hour, the accommodation ranges of yellow lines and blue lines are 0-517.56 MW and 27.28-570.26 MW, respectively.

C. Comparisons with Traditional RO Method

To compare the proposed method and the traditional RO [5], [14], we first give the optimal investment plans using the traditional RO method in Table III. Furthermore, we compare the out-of-sample performances of the proposed DRO method and the traditional RO method as shown in Fig. 5.

TABLE III
OPTIMAL INVESTMENT PLANS FOR GARVER 6-BUS SYSTEM WITH TRADITIONAL RO METHOD

δ	Corridor (number of newly-built lines)	Cost (k$)
105000	1-5 (1), 2-3 (3), 2-6 (6), 3-5 (2), 4-6 (3)	7800
500000	1-5 (1), 2-3 (3), 2-6 (6), 3-5 (2), 4-6 (4)	8400
1000000	1-4 (1), 1-5 (1), 2-3 (3), 2-6 (6), 3-5 (2), 4-6 (5)	10200

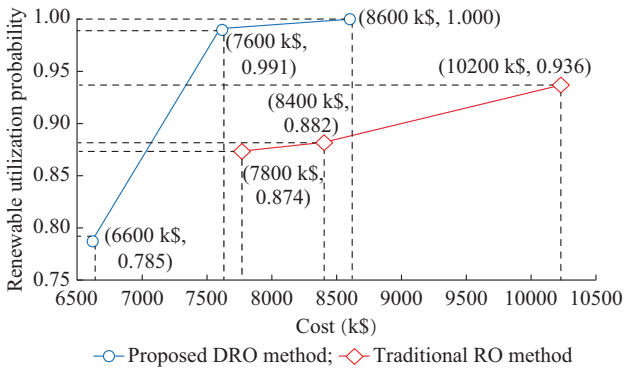

Fig. 5. Out-of-sample results of renewable utilization probability versus cost for Garver 6-bus system.

On one hand, when the investment cost goes up, the renewable utilization probability increases. For instance, at the cost of 6600 k$, the renewable utilization probability with the proposed DRO method is 0.785, which interprets that when we spend 6600 k$ on transmission network expansion, the renewable fully utilization probability for the system is 0.785. In other words, the system takes a risk with a probability of 0.215 to take emergency regulations, such as load shedding or wind power curtailment, to completely accommodate the wind generation outputs. On the other hand, the traditional RO method shows its conservativeness in that with a lower utilization probability, the RO method requires a higher investment cost compared with the proposed method. For instance, with the proposed DRO method, the system needs to spend 7600 k$ to obtain the utilization probability of 0.991, while with RO method, the system needs to pay 7800 k$ to obtain the utilization probability of 0.874. This is because the proposed DRO method considers the expectation of the worst-case probability distribution rather than the single worst-case scenario used in the RO method. In this context, the proposed method is less conservative than the traditional RO method.

D. Realistic Example: IEEE 118-bus System

We use a modified IEEE 118-bus system to verify the effectiveness of the proposed method. As shown in Fig. 6, the IEEE 118-bus system contains 19 generators, 35 synchronous condensers, 186 lines, 9 transformers, and 91 loads. Besides, two wind farms with an identical installed capacity of 300 MW are located at buses 32 and 88, respectively. In Fig. 6, the 30 candidate corridors are red. The initial parameters are from MATPOWER 7.1. The length of each transmission corridor is assumed to be the floored integral part of 250 times the corresponding reactance. The coefficients of the demands and wind generation outputs are shown in Appendix A. Other settings of the testing parameters keep the same as those in the Garver 6-bus system.

Like the Garver 6-bus system, when δ increases, more new lines will be built, thereby yielding higher investment costs, as can be observed from Table IV. This is because δ represents the weight factor for renewable utilization, which is regarded as the willingness of the system to fully accommodate wind generation outputs.

The trade-off between investment cost and accommodation ranges for IEEE 118-bus system is shown in Fig. 7. It is shown that when we increase investment costs, the accommodation ranges of renewable energy grow. At the 15th hour, the accommodation ranges corresponding to different investment costs of 20 k$, 360 k$, and 700 k$ are 51.15-391.61 MW, 25.99-405.25 MW, and 0-422.10 MW, respectively. Furthermore, we can observe from Fig. 8, that when the investment cost goes up, the renewable utilization probability increases. For example, at the cost of 20 k$, the renewable utilization probability is 0.85, which interprets that when we spend 20 k$ on transmission network expansion, the renewable full utilization probability for the system is 0.85.

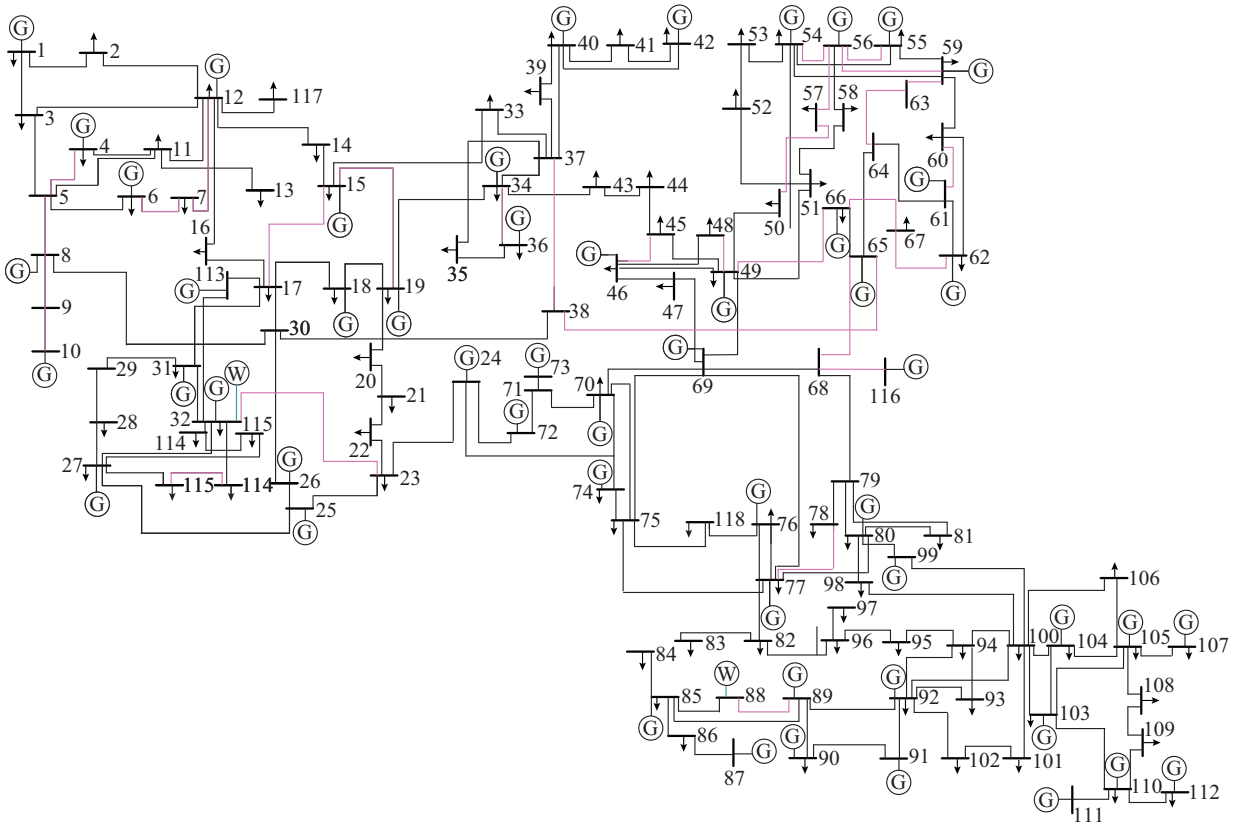

Fig. 6. Topology of IEEE 118-bus system.

TABLE IV
OPTIMAL INVESTMENT PLANS FOR IEEE 118-BUS SYSTEM

δ	Corridors (number of newly-built lines)	Cost (k$)
4000	68-116 (1)	20
5000	68-116 (1), 21-22 (1)	360
100000	68-116 (1), 21-22 (2)	700

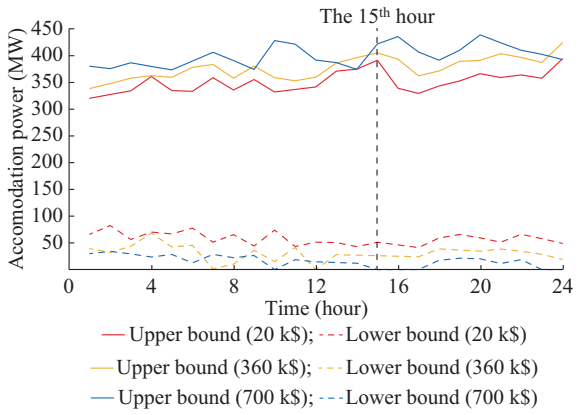

Fig. 7. Trade-off between investment cost and accommodation ranges for IEEE 118-bus system.

V. CONCLUSION

In this paper, we develop a DRO-based co-optimization model for the TNEP, yielding the minimum investment cost and the maximum penetration level of renewable generation.

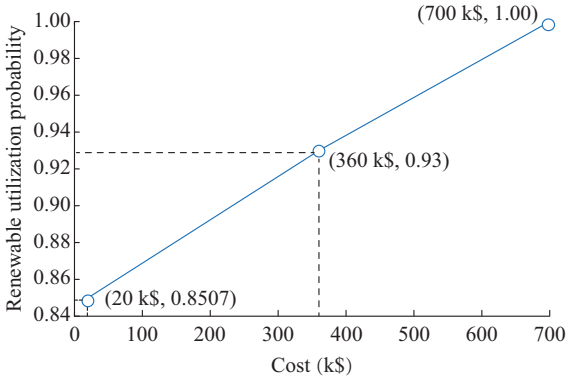

Fig. 8. Out-of-sample results of renewable utilization probability versus cost for IEEE 118-bus system.

The proposed model is characterized by a two-stage decision framework with variable bounds of the uncertain sets and distributionally robust joint chance constraints, which are hard to solve.

By applying the affine decision rule, second-order conic reformulation, and duality techniques, we reformulate the problem into a single-stage robust model, which is an MISOCP problem and is efficiently solved by commercial solvers. The case study shows that the proposed method explicitly quantifies the penetration level of renewable generation instead of implicitly setting them as constraints, which is intuitive for reference. Compared with the traditional RO method, the proposed method significantly improves conservativeness. An explicit trade-off between the cost and the

penetration level is expected to give the system planners a clear guideline for transmission network expansion planning under a high penetration level of renewable generation.

APPENDIX A

In Appendix A, we give the reformulation about the distributionally robust joint chance constraints (14). More details can be found in [39].

The ambiguity set (12) satisfies assumption (A1) in [41], and the distributionally robust joint chance constraint (13) can be expressed by its Bonferroni approximation.

$$\begin{cases} \inf\limits_{\mathbb{P}_{k,t}\in\mathcal{D}_{k,t}} \mathbb{P}_{k,t}(\xi_{k,t}\in[\xi_{k,t}^{\mathrm{L}},\xi_{k,t}^{\mathrm{U}}])\geq 1-g_{k,t} \quad \forall k\in\mathcal{K},\forall t\in\mathcal{T} \\ \sum\limits_{k\in\mathcal{K}} g_{k,t}\leq 1-u \quad \forall t\in\mathcal{T} \\ g_{k,t}\geq 0 \quad \forall k\in\mathcal{K},\forall t\in\mathcal{T} \end{cases} \tag{A1}$$

The equivalent formulation of (A1) is given as:

$$\inf_{\mathbb{P}_{k,t}\in\mathcal{D}_{k,t}} \mathbb{P}_{k,t}(|\xi_{k,t}-\mu_{k,t}|\leq \min(\mu_{k,t}-\xi_{k,t}^{\mathrm{L}},\xi_{k,t}^{\mathrm{U}}-\mu_{k,t}))\geq 1-g_{k,t} \quad \forall k\in\mathcal{K},\ \forall t\in\mathcal{T} \tag{A2}$$

Due to (A1), we have $1-g_{k,t}\geq u>2/3$. Then, by the Gauss inequality, we reformulate (A2) as:

$$1-\frac{4}{9\kappa_{k,t}^2}\geq 1-s_{k,t} \quad \forall k\in\mathcal{K},\ \forall t\in\mathcal{T} \tag{A3}$$

$$\kappa_{k,t}:=\frac{\min(\mu_{k,t}-\xi_{k,t}^{\mathrm{L}},\xi_{k,t}^{\mathrm{U}}-\mu_{k,t})}{\sigma_{k,t}} \quad \forall k\in\mathcal{K},\ \forall t\in\mathcal{T} \tag{A4}$$

Due to (A3), we have $s_{k,t}\kappa_{k,t}^2\geq 4/9$. Then, by introducing the auxiliary variables $v_{k,t}$ and $z_{k,t}$, we recast $s_{k,t}\kappa_{k,t}^2\geq 4/9$ as second-order conic constraints (24)-(29).

The formulas (24) - (29) are the reformulations of constraint (13).

REFERENCES

[1] M. Mahdavi, C. S. Antunez, M. Ajalli *et al.*, "Transmission expansion planning: literature review and classification," *IEEE Systems Journal*, vol. 13, no. 3, pp. 3129-3140, Sept. 2019.

[2] C. Roldan, R. Minguez, R. G. Bertrand *et al.*, "Robust transmission network expansion planning under correlated uncertainty," *IEEE Transactions on Power Systems*, vol. 34, no. 3, pp. 2071-2082, Dec. 2019.

[3] M. Alraddadi, A. J. Conejo, and R. M. Lima, "Expansion planning for renewable integration in power system of regions with very high solar irradiation," *Journal of Modern Power Systems and Clean Energy*, vol. 9, no. 3, pp. 485-494, May 2021.

[4] Y. Liu, R. Sioshansi, and A. J. Conejo, "Multistage stochastic investment planning with multiscale representation of uncertainties and decisions," *IEEE Transactions on Power Systems*, vol. 33, no. 1, pp. 781-791, Jan. 2018.

[5] X. Zhang and A. J. Conejo, "Robust transmission expansion planning representing long- and short-term uncertainty," *IEEE Transactions on Power Systems*, vol. 33, no. 2, pp. 1329-1338, Mar. 2018.

[6] A. Lotfjou, Y. Fu, and M. Shahidehpour, "Hybrid AC/DC transmission expansion planning," *IEEE Transactions on Power Delivery*, vol. 27, no. 3, pp. 1620-1628, Jul. 2012.

[7] H. Park and R. Baldick, "Transmission planning under uncertainties of wind and load: sequential approximation approach," *IEEE Transactions on Power Systems*, vol. 28, no. 3, pp. 2395-2402, Aug. 2013.

[8] J. Zhan, W. Liu, and C. Y. Chung, "Stochastic transmission expansion planning considering uncertain dynamic thermal rating of overhead lines," *IEEE Transactions on Power Systems*, vol. 34, no. 1, pp. 432-443, Jan. 2019.

[9] J. Li, L. Ye, Y. Zeng *et al.*, "A scenario-based robust transmission network expansion planning method for consideration of wind power uncertainties," *CSEE Journal of Power and Energy Systems*, vol. 2, no. 1, pp. 11-18, Mar. 2016.

[10] H. Mavalizadeh, A. Ahmadi, F. H. Gandoman *et al.*, "Multiobjective robust power system expansion planning considering generation units retirement," *IEEE Systems Journal*, vol. 12, no. 3, pp. 2664-2675, Sept. 2018.

[11] A. Arabali, M. Ghofrani, M. Etezadi-Amoli *et al.*, "A multi-objective transmission expansion planning framework in deregulated power systems with wind generation," *IEEE Transactions on Power Systems*, vol. 29, no. 6, pp. 3003-3011, Nov. 2014.

[12] F. D. Munoz, B. F. Hobbs, J. L. Ho *et al.*, "An engineering-economic approach to transmission planning under market and regulatory uncertainties: WECC case study," *IEEE Transactions on Power Systems*, vol. 29, no. 1, pp. 307-317, Jan. 2014.

[13] K. Tian, W. Sun, and D. Han, "Strategic investment in transmission and energy storage in electricity markets," *Journal of Modern Power Systems and Clean Energy*, vol. 10, no. 1, pp. 179-191, Jan. 2022.

[14] B. Chen and L. Wang, "Robust transmission planning under uncertain generation investment and retirement," *IEEE Transactions on Power Systems*, vol. 31, no. 6, pp. 5144-5152, Nov. 2016.

[15] H. Park, R. Baldick, and D. P. Morton, "A stochastic transmission planning model with dependent load and wind forecasts," *IEEE Transactions on Power Systems*, vol. 30, no. 6, pp. 3003-3011, Nov. 2015.

[16] A. Moreira, G. Strbac, R. Moreno *et al.*, "A five-level MILP model for flexible transmission network planning under uncertainty: a min-max regret approach," *IEEE Transactions on Power Systems*, vol. 33, no. 1, pp. 486-501, Jan. 2018.

[17] J. Li, Z. Li, F. Liu *et al.*, "Robust coordinated transmission and generation expansion planning considering ramping requirements and construction periods," *IEEE Transactions on Power Systems*, vol. 33, no. 1, pp. 268-280, Jan. 2018.

[18] Z. Zhou, C. He, T. Liu *et al.*, "Reliability-constrained AC power flow-based co-optimization planning of generation and transmission systems with uncertainties," *IEEE Access*, vol. 8, pp. 194218-194227, Oct. 2020.

[19] L. Baringo and A. Baringo, "A stochastic adaptive robust optimization approach for the generation and transmission expansion planning," *IEEE Transactions on Power Systems*, vol. 33, no. 1, pp. 792-802, Jan. 2018.

[20] A. Moreira, A. Street, and J. M. Arroyo, "An adjustable robust optimization approach for contingency-constrained transmission expansion planning," *IEEE Transactions on Power Systems*, vol. 30, no. 4, pp. 2013-2022, Jul. 2015.

[21] S. Dehghan and N. Amjady, "Robust transmission and energy storage expansion planning in wind farm-integrated power systems considering transmission switching," *IEEE Transactions on Sustainable Energy*, vol. 7, no. 2, pp. 765-774, Apr. 2016.

[22] F. Verástegui, A. Lorca, D. E. Olivares *et al.*, "An adaptive robust optimization model for power systems planning with operational uncertainty," *IEEE Transactions on Power Systems*, vol. 34, no. 6, pp. 4606-4616, Nov. 2019.

[23] M. Majidi-Qadikolai and R. Baldick, "Stochastic transmission capacity expansion planning with special scenario selection for integrating *N*−1 contingency analysis," *IEEE Transactions on Power Systems*, vol. 31, no. 6, pp. 4901-4912, Nov. 2016.

[24] A. Moreira, D. Pozo, A. Street *et al.*, "Reliable renewable generation and transmission expansion planning: co-optimizing system's resources for meeting renewable targets," *IEEE Transactions on Power Systems*, vol. 32, no. 4, pp. 3246-3257, Jul. 2017.

[25] A. Baharvandi, J. Aghaei, T. Niknam *et al.*, "Bundled generation and transmission planning under demand and wind generation uncertainty based on a combination of robust and stochastic optimization," *IEEE Transactions on Sustainable Energy*, vol. 9, no. 3, pp. 1477-1486, Jul. 2018.

[26] W. Wang, M. Wang, X. Han *et al.*, "Distributionally robust transmission expansion planning considering uncertainty of contingency probability," *Journal of Modern Power Systems and Clean Energy*. doi: 10.35833/MPCE.2020.000768

[27] J. Zhan, C. Y. Chung, and A. Zare, "A fast solution method for stochastic transmission expansion planning," *IEEE Transactions on Power Systems*, vol. 32, no. 6, pp. 4684-4695, Nov. 2017.

[28] R. Minguez, R. Garcia-Bertrand, J. M. Arroyo *et al.*, "On the solution of large-scale robust transmission network expansion planning under uncertain demand and generation capacity," *IEEE Transactions on Power Systems*, vol. 33, no. 2, pp. 1242-1251, Mar. 2018.

[29] J. Yan, B. Hu, K. Xie *et al.*, "Data-driven transmission defense planning against extreme weather events," *IEEE Transactions on Smart*

Grid, vol. 11, no. 3, pp. 2257-2270, May 2020.
[30] A. Hajebrahimi, I. Kamwa, E. Delage *et al.*, "Adaptive distributionally robust optimization for electricity and electrified transportation planning," *IEEE Transactions on Smart Grid*, vol. 11, no. 5, pp. 4278-4289, Sept. 2020.
[31] Y. Guo, K. Baker, E. Dall'Anese *et al.*, "Data-based distributionally robust stochastic optimal power flow – Part I: methodologies," *IEEE Transactions on Power Systems*, vol. 34, no. 2, pp. 1483-1492, Mar. 2019.
[32] Y. Guo, K. Baker, E. Dall'Anese *et al.*, "Data-based distributionally robust stochastic optimal power flow – Part II: case studies," *IEEE Transactions on Power Systems*, vol. 34, no. 2, pp. 1493-1503, Mar. 2019.
[33] A. Bagheri, J. Wang, and C. Zhao, "Data-driven stochastic transmission expansion planning," *IEEE Transactions on Power Systems*, vol. 32, no. 5, pp. 3461-3470, Sept. 2017.
[34] A. Bagheri, C. Zhao, F. Qiu *et al.*, "Resilient transmission hardening planning in a high renewable penetration era," *IEEE Transactions on Power Systems*, vol. 34, no. 2, pp. 873-882, Mar. 2019.
[35] A. Velloso, D. Pozo, and A. Street, "Distributionally robust transmission expansion planning: a multi-scale uncertainty approach," *IEEE Transactions on Power Systems*, vol. 35, no. 5, pp. 3353-3365, Sept. 2020.
[36] D. Alvarado, A. Moreira, R. Moreno *et al.*, "Transmission network investment with distributed energy resources and distributionally robust security," *IEEE Transactions on Power Systems*, vol. 34, no. 6, pp. 5157-5168, Nov. 2019.
[37] A. Bagheri and C. Zhao, "Distributionally robust reliability assessment for transmission system hardening plan under $N-k$ security criterion," *IEEE Transactions on Reliability*, vol. 68, no. 2, pp. 653-662, Jun. 2019.
[38] J. Zhao, T. Zheng, and E. Litvinov, "Variable resource dispatch through do-not-exceed limit," *IEEE Transactions on Power Systems*, vol. 30, no. 2, pp. 820-828, Mar. 2015.
[39] H. Ma, R. Jiang, and Z. Yan, "Distributionally robust co-optimization of power dispatch and do-not-exceed limits," *IEEE Transactions on Power Systems*, vol. 35, no. 2, pp. 887-897, Mar. 2020.
[40] R. Villasana, L. L. Garver, and S. J. Salon, "Transmission network planning using linear programming," *IEEE Power Engineering Review*, vol. PER-5, no. 2, pp. 36-37, Feb. 1985.
[41] W. Xie, S. Ahmed, and R. Jiang, "Optimized Bonferroni approximations of distributionally robust joint chance constraints," *Mathematical Programming*, vol. 2019, pp. 1-32, Nov. 2019.

Jingwei Hu received the B.E. degree in electrical engineering from Southeast University, Nanjing, China, in 2017. She is currently pursuing the Ph.D. degree in electrical engineering in Shanghai Jiao Tong University, Shanghai, China. Her research interests include power system optimization and renewable energy integration.

Xiaoyuan Xu received the B.S. and Ph.D. degrees both in electrical engineering from Shanghai Jiao Tong University, Shanghai, China, in 2010 and 2016, respectively. He was a Visiting Scholar with the Robert W. Galvin Center for Electricity Innovation, Illinois Institute of Technology, Chicago, USA, from 2017 to 2018. He is currently an Assistant Professor with Shanghai Jiao Tong University. His research interests include power system uncertainty quantification and power system optimization.

Hongyan Ma received the B.S. degree in electrical engineering from Shandong University, Jinan, China, in 2013 and the Ph.D. degree in electrical engineering from Shanghai Jiao Tong University, Shanghai, China, in 2019. She is currently an Assistant Professor in College of Information Science and Technology at Donghua University, Shanghai, China. Her research interests include power system operation, optimization, and renewable energy integration.

Zheng Yan received the B.S. degree from Shanghai Jiao Tong University, Shanghai, China, in 1984, and the M.S. and Ph.D. degrees from Tsinghua University, Beijing, China, in 1987 and 1991, respectively, all in electrical engineering. He is a Professor of electrical engineering from Shanghai Jiao Tong University. His current research interests include application of optimization theory to power systems, electricity markets, and dynamic security assessment.